Neurocomputing 160 (2015) 308–318

Contents lists available at ScienceDirect

Neurocomputing

journal homepage: www.elsevier.com/locate/neucom

Basis for the implementation of an EEG-based single-trial binary brain computer interface through the disgust produced by remembering unpleasant odors

Giuseppe Placidi [a,*], Danilo Avola [a], Andrea Petracca [a], Fiorella Sgallari [b], Matteo Spezialetti [a]

[a] Department of Life, Health and Environmental Sciences, University of L'Aquila, Via Vetoio, 67100, L'Aquila, Italy
[b] Department of Mathematics, University of Bologna, Piazza di Porta San Donato 5, 40126, Bologna, Italy

ARTICLE INFO

Article history:
Received 12 May 2014
Received in revised form
17 November 2014
Accepted 12 February 2015
Communicated by: S. Hu
Available online 23 February 2015

Keywords:
BCI
EEG
Human–computer interface
Disgust
Unpleasant odor
Emotion

ABSTRACT

In order to implement an EEG-based brain computer interface (BCI), a very large number of strategies (ranging from sensory–motor, p300, auditory based, visually based) can be used. However, no technique exists which is based on the olfactory stimulation or, better, based on the imagination of olfactory stimuli.

The present paper describes an innovative paradigm, that is the voluntary brain activation with the disgust produced by remembering unpleasant odors, and a simple and robust classification method on which a single trial binary BCI can be implemented. In order to classify the signal, mainly the channels P4, C4, T8 and P8 have been used, by spanning the frequency band between 32 and 42 Hz, that is a subset of the gamma band external to the bands usually occupied by other tasks (the interval between 1 and 30 Hz), and the alpha band between 8 and 12 Hz.

Right hemisphere of the brain and gamma band of frequencies are particularly sensitive when experiencing negative emotions, such as the disgust produced by smelling or remembering unpleasant odors, while the alpha band is usually modified with concentration. This constitutes an advantage for the proposed classification technique because it is made intrinsically easy by the localization into particular positions and frequencies: different features are mostly based on different frequency bands.

The choice of disgust produced by remembering unpleasant odors is twofold: smelling is an ancestral sensation which is so strong that its EEG signal is produced also in persons affected by hyposmia when they imagine an olfactory situation; it can be used without external stimulation, that is the user can decide freely when and if activate it.

The proposed method and the experimental setup are described and a series of experimental measurements are presented and discussed. The accuracy of the proposed method is also evaluated and the reached levels are about 90%. The proposed system can be a useful communication alternative for disabled people that cannot use other BCI paradigms.

1. Introduction

A BCI is a computer-based communication system that collects signals generated by voluntary neural activity of the Central Nervous System (CNS) and its goal is to provide a new channel of output for the brain that requires voluntary adaptive control by the user [1,2]. EEG is the technique used to measure these signals by placing electrodes outside the skull [3], gives immediate responses (high temporal resolution), is easy to use, safe, inexpensive and, for these reasons, is effective to measure brain activity in a common BCI.

The collected EEG signal can be divided into several bands of frequency corresponding to different coarse activities. Delta band activity, up to 3 Hz, is mainly seen in deep sleep. Theta band (4–7 Hz) is often observed with drowsiness or meditation. Alpha band (8–12 Hz) is seen when people are awake, more apparent when eyes are open, and a power decreasing is observed when people engage in active processing and concentration [4]. Beta band (13–30 Hz) is apparent with active thinking or concentration. Finally, gamma band (30–100 Hz) is involved in a series of cognitive processes, but new hypotheses [5,6] relates gamma oscillations to three underlying processes: the comparison of memory contents with stimulus-related information, the utilization of signals derived from this comparison, and the presence of emotional states. Modifications occur mainly around 40 Hz.

* Corresponding author. Tel.: +39 862433493; fax: +39 862433633.
E-mail address: giuseppe.placidi@univaq.it (G. Placidi).

http://dx.doi.org/10.1016/j.neucom.2015.02.034
0925-2312/

A good part of communication BCIs for disabled people [7] is based on event-related signals induced by external stimuli and synchronized with them (an example is the P300 [8]). Another consistent part is based on sensory–motor rhythm amplitudes [9–11]. For patients with impaired vision, or suffering from seizures attacks caused by too fast visual stimuli such those used in P300, or that have never experienced the control of the motor part of their body (they never knew what it means to move a limb), or whose signals produced by sensory–motor rhythms, mostly at the alpha band, can be easily confused with those due to artifacts caused by involuntary and frequent movements, other paradigms, such as auditory [12–14] and tactile [15,16], have been explored. However, cases in which also these paradigms have little or no effect are frequent [13]. For this reason, new ways have to be explored and one of the most promising could be that of BCI based on measuring the voluntary brain activity produced by emotions [5,17,18].

Emotions have been first explored in the field of affective computing where some fascinating studies are dedicated in making the computer more empathic to the user and involved the measurement of the user's emotions and to represent them into human–computer interaction systems [19]. Their aim is to find the activation of specific brain regions in responses to specific emotions but, while some regions are more active than others when experiencing specific emotions, no specific region is activated by a single emotion [20,21]. In fact, the brain regions most responsible for emotions are amygdala, insula, anterior cingulate cortex, and orbitofrontal cortex [22]. By using fMRI, recently it has been found that there exist specific patterns of brain activity, i.e. groups of brain zones, related to specific emotions and that these patterns are common across individuals [23].

Though these advances, it remains very difficult to differentiate between different emotions, especially across individuals, because their patterns are very similar and can be confused each other and because they are also subjective (i.e. different individuals can have different ways to deal with emotions). Moreover, complex multi-voxel pattern analysis techniques have to be used to identify distributed patterns associated with specific emotions [24]. In addition to that, EEG is still poorly used to classify emotions. Choppin [25] used neural networks to classify EEG signals from three emotions and got 64% classification accuracy. Chanel et al. [26] also confirmed that EEG and other physiological signals can be used to recognize emotions and obtained a classification accuracy between 60% and 70%, very similar to that obtained by Bos [27] or by Zhang et al. [28]. Wang et al. [29], by using advanced machine learning classification approaches, obtained accuracy above 90%. However, the previously listed works based the recognition of emotions that were artificially elicited through visual stimuli. The best would be to recognize a self-induced emotional state, without any sort of external elicitation, to autonomously drive a BCI system.

A possible solution, offered by psycho-physiological research, has shown that a more active left frontal region indicates a positive reaction, and a more active right lobe indicates a negative effect [30,31]. This makes negative emotions well distinguishable from positive emotions. This is also confirmed in [23] where the authors, by performing inter-emotion comparisons, located one of the negative emotions, the disgust, in the opposite side with respect to positive emotions, for example happiness. Between these two emotions, the disgust, especially produced by an unpleasant odor, seems to be stronger than happiness at least when looking at its effects: vomit, increased sweating, heart rate and chills. Moreover, its manifestation, related to the activation of the right lobe is distinguishable from other mental tasks that like positive emotions, tend to activate preferentially the left frontal region of the brain. Finally, the disgust is supposed to be a particular, unnatural and infrequent state of a person while, on the contrary, it is supposed that happiness be the usual state. In this case, it would be easier to recognize the disgust as a consciously activated state to perform a choice with respect to happiness.

This would suggest that disgust can be used as a driving system for an effective BCI, a binary BCI, where disgust (indicating YES, or 1) has to be differentiated from the rest (indicating NO, or 0) to allow very high accuracy. But how to elicit disgust? Is it necessary an external source or a self-induced procedure could be sufficient?

Disgust can be elicited in different ways: by listening sounds, by viewing videos or pictures, by smelling stinking odors or, more interestingly, by remembering such disgusting situations [32,33]. Regarding the case of remembering smelling stinking odors, it has been demonstrated with fMRI [32] that in patients with congenital hyposmia, which had never been able to recognize odors, the brain responded even when they imagined odors. Moreover, the regions of the brain activated by odors in patients with congenital hyposmia were similar to those in the other groups, though the degree of activation was about 15% of that in subjects with a normal sense of smell. Therefore, in these patients brain activation occurs also just by imagining an odor. This is also more noticeable in subjects with a normal sense of smell: once an odor has been experienced, odor imagination is present, recallable, and capable of inducing a relatively constant degree of brain activation even in the absence of the ability to recognize an actual corresponding odor. This particularity can be used to produce brain activation both due to pleasant and to unpleasant odors. Being pleasant odors linked to positive emotions and unpleasant odors linked to negative emotions, in particular to disgust, a brain asymmetry is found when decoding pleasant versus unpleasant odors (left hemisphere shows greater efficiency for the decoding of pleasant odors, right hemisphere shows greater efficiency for the decoding of unpleasant odors) [34].

Obviously, a direct elicitation would produce greater signals than an imagined situation but, for a direct elicitation external, mechanically driven, cumbersome, uncomfortable, and annoying sources would be necessary, that leaves no room for free choices. On the contrary, imagining a disgusting situation is a self-induced procedure that can be, in principle, freely used to perform a choice, when desired, involving the right hemisphere of the brain. These considerations suggested us the possibility of implementing a spatial-frequency (spatial referred mainly to the right hemisphere of the brain; frequency, referred to the gamma and to the alpha bands of frequencies) filter to be used in a self-induced disgust-based EEG-BCI. The temporal synchronization could be given by a repetitive (maybe audio-visual) interface to suggest different possibilities to choose from. For this reason, in the present paper we describe the classification strategy that can be used to recognize the EEG signal modifications due to an auto induced, voluntary, disgust produced by remembering unpleasant odors.

The aim is to give the basis for a binary BCI, based on the recognition of an atavistic emotion, like disgust, produced by an atavistic sense, like olfaction, without using any external elicitation but imagining a previously experienced disgusting odor autonomously elicited. It is important to note that, though a double status can, in principle, be assumed (also by imagining pleasant odors), is difficult to switch between two activations without getting tired and without creating confusion to the classification method (other tasks could be confused with positive emotions involving the left brain hemisphere). For this reason, and to simplify the model, the binary and single-trial EEG-BCI we imagine is based on remembering an unpleasant odor to say YES, otherwise it is supposed that NO is chosen.

The manuscript is structured as follows: Section 2 details the acquisition paradigm; Section 3 describes data analysis and classification strategy; Section 4 reports and discusses experimental results, from data collected by 28 volunteers used to verify the effectiveness of the paradigm and to evaluate the classification accuracy; Section 5 contains conclusions and future work.

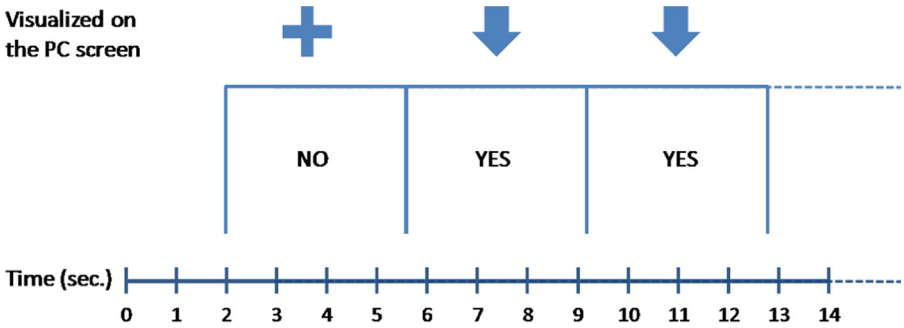

Fig. 1. Trial paradigm. Crosses and arrows are presented on the screen: the subject has to relax or remember a disgusting odor, respectively. Each symbol lasts for 3.6 s on the screen.

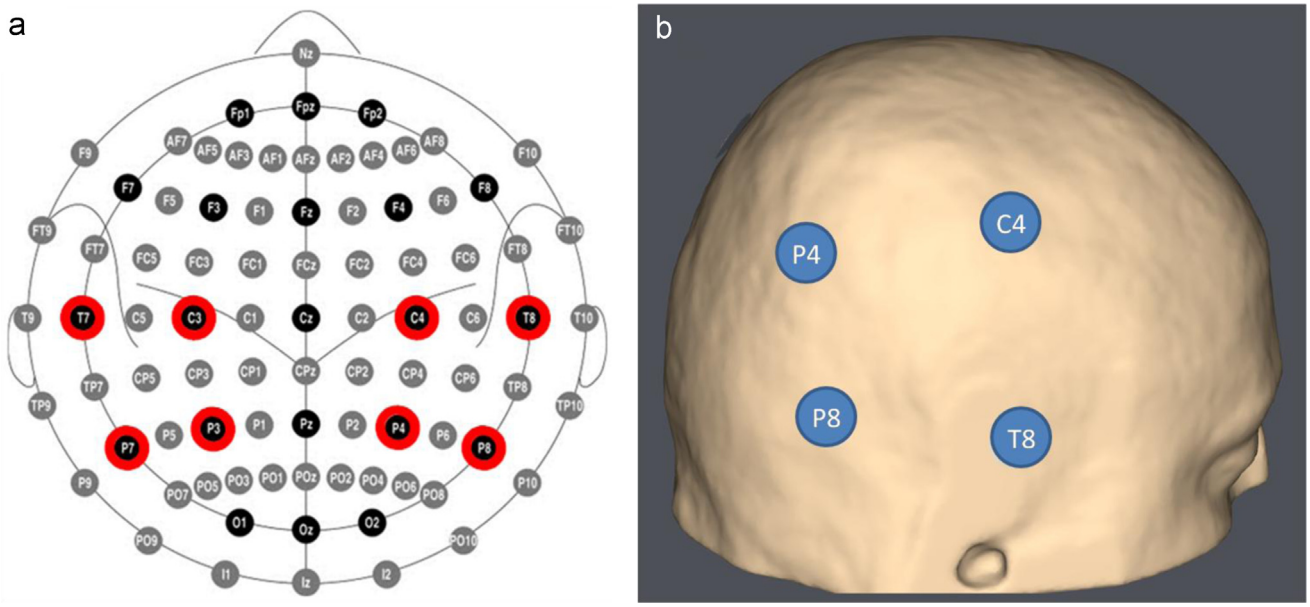

Fig. 2. Red circles (a) indicate the used positions of the electrodes of the Enobio[NE] equipment in the 10–20 international localization system. 3D localization (b) of the electrodes used by the classification strategy. (For interpretation of the references to color in this figure legend, the reader is referred to the web version of this article.)

2. The proposed acquisition paradigm

In order to verify that the disgust derived by remembering an unpleasant odor produces a specific EEG signal combination that can be easily recognized and classified, we analyzed EEG data from experiments conducted on 28 healthy subjects (18 men and 10 women, age: 36 ± 3.5), divided in 4 groups, each composed by 7 subjects. In the following we use the notation *Sx.y* to indicate the *y*th subject of the *x*th group (*x* represents the group and *y* represents the subject). Of the whole set of subjects, S1.3, S2.5, S3.2, S3.4, S3.5, S4.1 and S4.6 were left handed (5 men and 2 women).

The grouping of the subjects was random and its simple scope was to organize a temporal schedule for the experiments in different days. For this reason, data regarding the analyzed subjects were treated as allowing to a single, large, group.

During the experiment, the examined subject was sat in a comfortable armchair with the arms lying relaxed on the arms of the chair, in a quiet and lit room. The experiment consisted in showing a sequence of symbols "+" or "⇓", each presented for 3.6 s on a computer screen (Fig. 1). The order of presentation was random but the number of symbols "+" was equal to the number of symbols "⇓" and their sum was always the same. It is important to note that the scope of using these graphic sequences was just to synchronize the tasks and not to elicit the emotion. This is the reason why we choose anonymous symbols, that is not directly attributable to disgust or to relax. In the same time, we excluded the brain region responsible of processing visual information, the occipital channels, from classification (the occipital signals have not even been measured, as described see below).

Each subject was instructed to be relaxed (during the cross) or to remember an unpleasant odor (during the arrow). In the activated status (during the arrow), the subject had to remember a disgusting situation produced by an unpleasant odor. It is important to note that the disgust had to be produced by remembering a subjective unpleasant olfactory situation and not, for example, by remembering another disgusting situation (an image evoking disgust was acceptable if this was accompanied by a joint disgusting odor).

Moreover, being the proposed activation strategy also an imagination task that should involve the usage of the working memory area, we excluded the frontal channels to avoid influences of EEG signals coming from the frontal region, as done for the occipital channels responsible of visual information processing.

Two sequences containing 100 trials (50 trials for each class, where a class was associate to "+" and another to "⇓") were recorded for each subject. In each test (or sequence), the trials of the two classes were mixed in a random order, executed without interruptions for 12 min. The order of execution of the two tests was cyclic: from *Sx.*1 to *Sx.*7, for $x = 1.7$, respectively, with 18 min of interruptions between consecutive subjects (for preparation of the following subject), and another break of one hour between the two tests. In this way, each subject experienced a relaxing period of about 4.5 h between the first and the second test. The day before the tests, all subjects were summoned at the same time and received instructions, through the

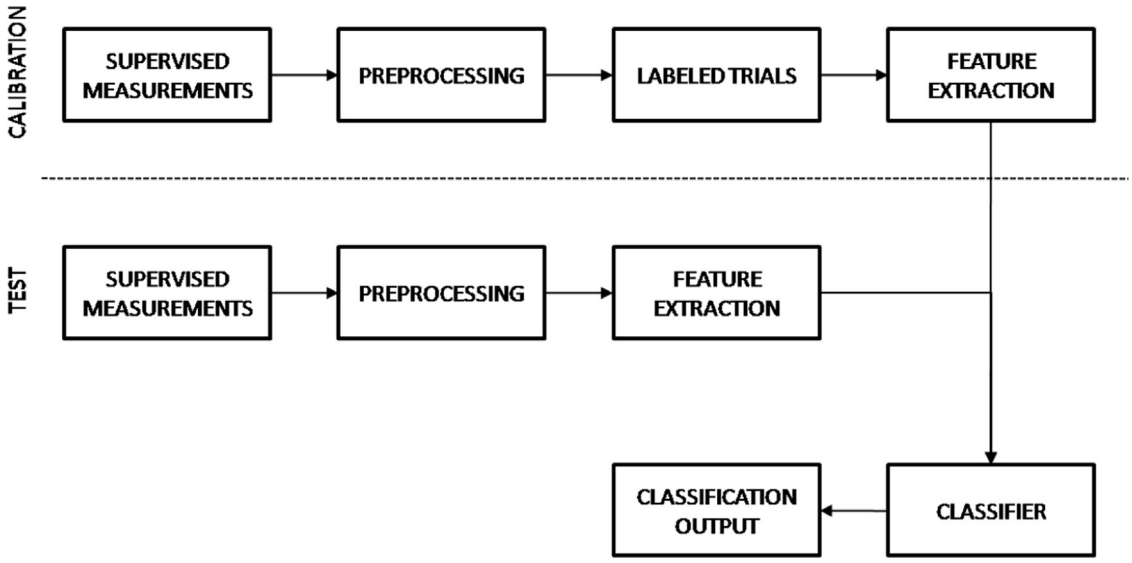

Fig. 3. Signal classification system. The system is first calibrated and then the collected signals are preprocessed and their features extracted and compared with those of the labeled trials stored after calibration.

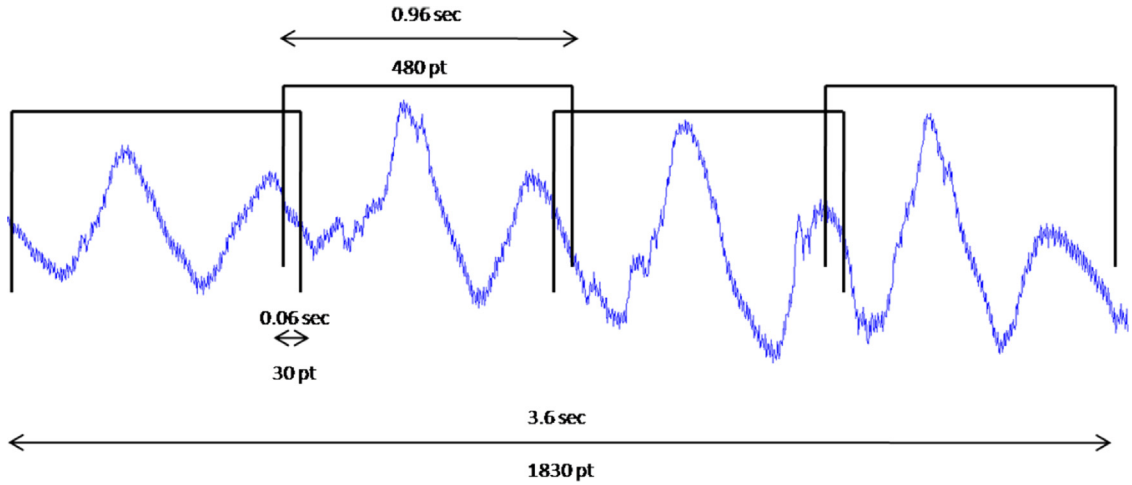

Fig. 4. Signal pre-processing scheme. Each signal, whose duration is 3.6 s, is broken into 4 pieces and the STFT is calculated on each piece after the elimination of a linear trend. The considered pieces have a common, overlapping, zone (30 sampled points, corresponding to 0.06 s).

projection of a brief video, on the modality and duration of the tests. At the end of the driven instruction procedure, the subjects were encouraged to ask and discuss what remained still unclear and, finally, were summoned for the next day, separately, 30 min from each other.

The system used to record the EEG was Enobio$^{NE®}$ [35], an 8 channels (two more channels are used one as reference and another for ground) precise and robust wireless EEG equipment that uses a neoprene cap to fix the channels in the desired brain locations. Thanks to the supporting software, the channels can be dynamically associated to variable positions in the international 10–20 system [36]. The channels of the 10–20 international system we used were the following: P4, C4, T8, P8, P3, C3, T7 and P7 (Fig. 2a). As will be clarified below, signals from the channels P3, C3, T7 and P7 had a limited use for the classification strategy: these signals were used just for confirmation of the classification choice.

We used dry copper electrodes (coated by a silver layer) fixed to the cap that ensured the contact with the subject's scalp. The electric conduction was ensured just by contact: the electrodes terminated with a circular series of contact tips to pass through the hair. For the reference and ground channels, located just behind the right ear in a region not covered by the cap and by hair, the fixing strategy was ensured by adhesive, disposable, flat gel-containing connectors to whom the electrodes were plug in. Main features of Enobio$^{NE®}$ were: amplitude resolution of 24 bits (0.05 uV); sampling rate of 500 Hz; sampled signals were filtered between 1 Hz and 46 Hz; data were analyzed and classified by a specific algorithm (described below) implemented in Matlab® [37], by using the environment BCI2000 and its visualization utilities [38]. The BCI2000 software, in fact, contains the utilities to capture the signals directly from Enobio$^{NE®}$ and to process them with its internal functions.

3. Data analysis and classification

After an initial evaluation, signals were filtered with a band-pass filter to maintain just the frequencies between 8 and 12 Hz (demonstrating cerebral activity due to concentration) and between 30 and 42 Hz (demonstrating disgusting activity at the gamma band). Moreover, the only considered channels are P4, C4, T8 and P8, those mainly involved in remembering negative emotions, especially due to disturbing odors (Fig. 2b). It is important to note that, at an early processing phase, we also analyzed other frequency bands. In particular, we found some modifications in the beta band but these were very unstable because they changed many times both in amplitude and in frequency position during the same task in each subject. This behavior was observed in most of the examined

subjects. For this reason, and for the fact that the beta band is not considered to be peculiar for emotions, we completely excluded it from the analysis. The way the chosen bands were used in the classification strategy, and further reduced, are discussed below.

The strategy used to classify the signals was preceded by two phases (see Fig. 3): preprocessing and feature extraction, both for calibration and test (in the calibration step, a further phase, consisting in the labeling of some trials, was performed to indicate to whose signals corresponded YES and to whose corresponded NO).

The preprocessing phase consisted in the application of the Short Time Fourier Transform (STFT), i.e. the multiplication of a time window to the input signal before the calculation of the Fourier Transform, after the elimination of a trend from each windowed portion of the signal. The applied STFT was the following:

$$S(\omega,\tau)=\sum_{-\infty}^{\infty}\delta(x(t_k)w(t_k-\tau))e^{-i\omega t_k} \tag{1}$$

where S was the transformed signal, in the parameters ω (frequency) and τ (window position), t_k were the sampled points of a signal, and δ was a de-trend function (used to eliminate a linear trend from the windowed portion of the signal) necessary to eliminate leakage from the windowed signal (note that this operation would not modify the information content of the signal at the considered frequency bands). In our experiments, we used 4 partially overlapping windows to calculate the STFT (see Fig. 4). Each window was 0.96 s in duration (corresponding to 480 points at 500 Hz) and overlapped of 0.06 s with the nearest window (corresponding to 30 points at 500 Hz). In this way, we ensured a frequency resolution of about 1.04 Hz. We used STFT to maintain, of the whole time interval, the most similar periods and to perform the average on these similar data.

Data similarity between pieces of signals was evaluated by calculating the r^2, defined as follows [39,40]:

$$r_c^2(f)=\left(\frac{\sqrt{L_1L_2}}{L_1+L_2}\frac{\mu(X_{1c})-\mu(X_{2c})}{\sigma(X_{1c}\cup X_{2c})}\right)^2 \tag{2}$$

where X_{1c} and X_{2c} were the compared pieces of power spectra of the signal corresponding to the channel c and defined into a neighborhood $2\Delta f$ of f ($2\Delta f$ had to be not too wide to avoid loss of resolution, usually it is 3 or 5 Hz), L_1 and L_2 were the numbers of samples (in our case $L_1=L_2$), μ was the mean value, and σ the standard deviation. Large r^2 denoted low similarity (or, equivalently, high dissimilarity) between the considered pieces of signals. In the feature extraction phase of the calibration, the 4 pieces of the signal were compared: the worse piece of each signal, according to r^2, was discarded and the power spectra of the remaining pieces were averaged together. Signals coming from different channels were maintained separated. During calibration this operation was repeated on each signal, both for activations and for relaxations. For the whole set of activations, joint r^2 was calculated again: the 3 most similar power spectra were retained and averaged together and the worse was discarded. This process was repeated for each considered channel. The same procedure applied to the power spectra of the relaxing signals. At the end of the process, two resulting pieces remained for each channel, one for activation and one for non-activation, and the pieces corresponding to different channels, separately for activation and non-activation, were averaged together.

Aim of the previously described operations was to make the classification method robust against artifacts partially affecting the trial, such those present in the initial part of a trial and caused by the difficulty for a subject to switch instantly from a task to another (from a "+" to a "⇓" and vice-versa).

At this stage, r^2 was calculated again between these signals and one sub-interval of 5 Hz of frequencies was considered around the maximum value of r^2 occurring inside each of the considered bands. This operation was performed to refine the band selection, being this positioning very subjective (inter-subjects variability) and also varying with time in the same subject (intra-subject variability).

The maximum values of r^2 occurring inside each of these bands, and the absolute minimum of r^2, were also used to define two thresholds t_α and t_γ:

$$t_\alpha=1/2(\max(r_\alpha^2)-\min(r_\alpha^2)) \tag{3a}$$

$$t_\gamma=1/2\left(\max\left(r_\gamma^2\right)-\min\left(r_\gamma^2\right)\right) \tag{3b}$$

The previous threshold allowed the classification of the current signal. During calibration and by using Eqs. (1) and (2), signals from the channels in the left hemisphere of the brain were preprocessed in the same way used for the corresponding channels in the right hemisphere.

Besides that, for the excluded channels (left hemisphere) the parameter and p, a threshold value indicating the typical distance between activation and non-activation, was calculated as follows:

$$p=\sum_{c\in Excl.\ channels}\ \sum_{f\in Sampled\ Freq.\ 5\le f\le 46} r_c^2(f) \tag{4}$$

where r^2 was evaluated between activation and non-activation, c and f indexed the excluded channels and the sampled frequencies (the values 5 and 46 represented, in Hz, the lower and upper limit of the sum), respectively.

The classification strategy used for the collected data (signals from right hemisphere) measured for 3.6 s, can be summarized in the following steps:

For each channel

1. Calculate the STFT for the signal divided into 4, partially overlapping, pieces (Fig. 4);
2. Calculate the mutual r^2 of the resulting spectra to discard the worse piece and average the other pieces;

End;

3. Average the resulting spectra from different channels;
4. Compare the resulting spectra, by using r^2, with those registered in the calibration stage for the activation and the non-activation and classify the current dataset;
5. If step 4 classifies an activation, Eq. 4 is evaluated between the current dataset and the activation dataset stored during calibration. Let p_c be the resulting value;
6. If $p_c<p$, then the activation is confirmed, elsewhere the current dataset is corrupted (a false positive occurred) and has to be discarded;
7. Return.

Step 4 of the previous strategy is summarized in Table 1: one of the represented outcomes could occur for the considered dataset. The r^2 evaluation was from left to right of the table (that is, first the signal was compared with the activation signal, γ band before α band, and then with the non-activation signal). The first two rows of the table were the most frequent. However, due to the presence of noise on the collected signal, or to the modification of the conditions of the system (the EEG signal is strongly non stationary), or to an inconstant concentration of the subject on the assigned task, also other outcomes could be possible. In particular, the worst cases were those represented on rows 4 and 7 of Table 1 (clearly contradictory) and, in case of occurrence, the dataset should have been discarded and repeated when used in a real-time BCI. Obviously, also row 8 represented an edge situation. Rows 5 and 6 had these outcomes because the technique was driven by what happened in the γ band first. However, those limit cases, though treated, were expected to be

Table 1
Scheme of the classification method. The signal is first compared to the Activation data, both in the γ and in the α bands (columns 2 and 3) and then, if necessary, to the Non-Activation data in the same bands (columns 3 and 4). The column RESULT represents the consequence of each combination given in the corresponding row (A and NA represent Activation and Non-Activation, respectively). Void cells correspond to contradictions (the classification strategy is unable to decide between A and NA). In case of contradiction, data acquisition should be repeated in a real-time BCI.

	ACTIVATION (A)		NON ACTIVATION (NA)		RESULT
	γ	α	γ	α	
1	$r^2_{SA} \geq t_\gamma$	$r^2_{SA} \geq t_\alpha$	DON'T CARE	DON'T CARE	**NA**
2	$r^2_{SA} < t_\gamma$	$r^2_{SA} < t_\alpha$	DON'T CARE	DON'T CARE	**A (Verify at Step 5)**
3	$r^2_{SA} \geq t_\gamma$	$r^2_{SA} < t_\alpha$	$r^2_{SNA} \geq t_\gamma$	$r^2_{SNA} \geq t_\alpha$	**A (Verify at Step 5)**
4	$r^2_{SA} \geq t_\gamma$	$r^2_{SA} < t_\alpha$	$r^2_{SNA} \geq t_\gamma$	$r^2_{SNA} < t_\alpha$	
5	$r^2_{SA} \geq t_\gamma$	$r^2_{SA} < t_\alpha$	$r^2_{SNA} < t_\gamma$	DON'T CARE	**NA**
6	$r^2_{SA} < t_\gamma$	$r^2_{SA} \geq t_\alpha$	$r^2_{SNA} \geq t_\gamma$	DON'T CARE	**A (Verify at Step 5)**
7	$r^2_{SA} < t_\gamma$	$r^2_{SA} \geq t_\alpha$	$r^2_{SNA} < t_\gamma$	$r^2_{SNA} \geq t_\alpha$	
8	$r^2_{SA} < t_\gamma$	$r^2_{SA} \geq t_\alpha$	$r^2_{SNA} < t_\gamma$	$r^2_{SNA} < t_\alpha$	**NA**

Table 2
Summary of experimental results. For each subject (rows), the reported data indicate, for each test and for each class of trials (Activation or Non-Activation), the amount of trials recognized as Activation (A), Non-Activation (NA) or Not Recognized (columns indicated in gray and represented with a "?"). The optimal frequencies and the classification accuracy are also reported. Mean values and standard deviations of data in each column are also shown. Subjects labeled with (*) were left-handed.

SUB	TEST 1									TEST 2									$\Delta f\alpha$	$\Delta f\gamma$	ΔACC	TOTAL ACC.
	ACTIVATION TRIALS			NON ACTIVATION TRIALS			α	γ	ACC. (%)	ACTIVATION TRIALS			NON ACTIVATION TRIALS			α	γ	ACC. (%)				
	A	NA	?	A	NA	?				A	NA	?	A	NA	?							
S1.1	41	3	1	4	40	1	9,4	41,8	90,0	41	4	0	3	42	0	10,5	39,7	92,2	1,0	2,1	2,2	91,1
S1.2	37	7	1	3	42	0	8,4	33,5	87,8	41	4	0	5	40	0	8,4	33,5	90,0	0,0	0,0	2,2	88,9
S1.4	39	6	0	1	43	1	10,5	39,7	91,1	38	7	0	3	42	0	11,5	37,7	88,9	1,0	2,1	-2,2	90,0
S1.5	36	8	1	2	43	0	8,4	33,5	87,8	42	3	0	4	41	0	8,4	37,7	92,2	0,0	4,2	4,4	90,0
S1.6	38	5	2	6	36	3	8,4	37,7	82,2	33	11	1	2	42	1	9,4	39,7	83,3	1,0	2,1	1,1	82,8
S1.7	37	8	0	5	39	1	11,5	36,6	84,4	38	7	0	5	39	1	10,5	35,6	85,6	1,0	1,0	1,1	85,0
S2.1	42	3	0	5	40	0	9,4	40,8	91,1	42	3	0	3	42	0	9,4	40,8	93,3	0,0	0,0	2,2	92,2
S2.2	37	6	2	4	41	0	11,5	36,6	86,7	37	8	0	4	40	1	11,5	36,6	85,6	0,0	0,0	-1,1	86,1
S2.3	38	7	0	2	42	1	10,5	39,7	88,9	38	7	0	3	41	1	9,4	38,7	87,8	1,0	1,0	-1,1	88,3
S2.4	36	7	2	4	40	1	9,4	36,6	84,4	38	7	0	3	39	3	11,5	35,6	85,6	2,1	1,0	1,1	85,0
S2.6	42	3	0	1	44	0	9,4	35,6	95,6	42	3	0	2	43	0	8,4	35,6	94,4	1,0	0,0	-1,1	95,0
S2.7	38	6	1	4	41	0	11,5	41,8	87,8	41	4	0	4	41	0	11,5	38,7	91,1	0,0	3,1	3,3	89,4
S3.1	43	2	0	7	37	1	10,5	32,4	88,9	43	2	0	5	40	0	10,5	32,4	92,2	0,0	0,0	3,3	90,6
S3.3	42	2	1	3	41	1	9,4	35,6	92,2	43	1	1	3	41	1	9,4	33,5	93,3	0,0	2,1	1,1	92,8
S3.6	43	2	0	4	41	0	11,5	41,8	93,3	43	2	0	4	41	0	10,5	40,8	93,3	1,0	1,0	0,0	93,3
S3.7	40	4	1	4	40	1	11,5	37,7	88,9	40	4	1	6	38	1	11,5	35,6	86,7	0,0	2,1	-2,2	87,8
S4.2	42	2	1	2	42	1	11,5	40,8	93,3	42	2	1	1	44	0	11,5	41,8	95,6	0,0	1,0	2,2	94,4
S4.3	42	3	0	3	40	2	9,4	39,7	91,1	42	2	1	3	41	1	8,4	37,7	92,2	1,0	2,1	1,1	91,7
S4.4	40	4	1	3	40	2	10,5	34,5	88,9	41	3	1	5	40	0	11,5	36,6	90,0	1,0	2,1	1,1	89,4
S4.5	40	5	0	2	43	0	10,5	40,8	92,2	40	5	0	0	44	1	10,5	40,8	93,3	0,0	0,0	1,1	92,8
S4.7	38	6	1	8	37	0	9,4	39,7	83,3	40	4	1	8	37	0	8,4	41,8	85,6	1,0	2,1	2,2	84,4
S1.3*	38	6	1	4	40	1	8,4	38,7	86,7	41	4	0	4	39	2	9,4	39,7	88,9	1,0	1,0	2,2	87,8
S2.5*	41	2	2	3	42	0	10,5	35,6	92,2	42	1	2	1	44	0	10,5	36,6	95,6	0,0	1,0	3,3	93,9
S3.2*	36	9	0	1	43	1	9,4	34,5	87,8	37	7	1	1	42	2	9,4	32,4	87,8	0,0	2,1	0,0	87,8
S3.4*	41	4	0	4	38	3	10,5	32,4	87,8	40	5	0	5	40	0	9,4	32,4	88,9	1,0	0,0	1,1	88,3
S3.5*	36	9	0	3	40	2	8,4	41,8	84,4	36	8	1	4	41	0	8,4	40,8	85,6	0,0	1,0	1,1	85,0
S4.1*	38	7	0	1	44	0	10,5	33,5	91,1	42	3	0	4	41	0	10,5	32,4	92,2	0,0	1,0	1,1	91,7
S4.6*	36	8	1	3	40	2	8,4	34,5	84,4	36	9	0	4	41	0	9,4	33,5	85,6	1,0	1,0	1,1	85,0
MEAN	39,2	5,1	0,7	3,4	40,7	0,9	10,0	37,4	88,7	40,0	4,6	0,4	3,5	40,9	0,5	10,0	37,1	89,9	0,6	1,3	1,2	89,3
STD	2,3	2,3	0,7	1,7	2,0	0,9	1,1	3,1	3,3	2,5	2,5	0,6	1,7	1,7	0,8	1,1	3,1	3,5	0,6	1,0	0,2	3,3

rare. In principle, they should be impossible and, if occurring frequently, it could be the sign of one of the following situations:

1) the selected channels or the classification strategy or the selected frequency bands were not adequate;
2) the acquisition conditions were considerably changed and a new calibration is necessary;
3) the subject was no longer focused on the task.

Clearly, the first situation could occur ever, also immediately after a calibration (also indicated by the fact that the two classes, activation and non-activation, would be very close). On the contrary, the second situation could occur only when a long time interval elapsed after a calibration. In this second case, the method would have been effective.

Step 5 of the proposed algorithm would eliminate false positive activations. An apparent activation (false) could occur when external noise (caused for example by subject's movements, electromagnetic disturbances, etc.) heavily modified the EEG signals. In this case, modifications would modify both the used channels and the discarded channels, affecting all the frequency bands. For this reason, in the case of a presumed activation, the trial was compared with the activation stored in memory during the calibration phase, for all the frequencies and for those channels

where activation was supposed to have very limited effects. If the trial was clearly different from a standard activation (the integral of the r^2 function was greater than a value, considered as a threshold, calculated between a standard activation and a standard non activation during the calibration), probably external noise had significantly affected the signals and a false activation had occurred. Elsewhere the activation was confirmed.

4. Results

Data collected from the 28 treated subjects were analyzed by using the threshold classification algorithm described above. It is important to note that none of the treated subjects was discarded from the test and that, for each subject, all trials were classified and results included. For each test, the first 10 trials (5 arrows, or A, and 5 crosses, or NA) were used to calibrate the system and to calculate, for each subject, the optimal γ and α frequencies and the thresholds t_α and t_γ. The remaining trials were used to evaluate the accuracy of the system (calculated as the percentage of the rightly classified answers with respect to the total answers to be given) to test the classification performance.

Classification results are summarized in Table 2. In order to demonstrate that the brain activation was independent of being right-handed or left-handed, data were separated in right-handed and left-handed subjects not by order of experiments (the order and group of experiment is recognizable by the name assigned to the subjects, as explained above). For each subject, the accuracy was calculated for both tests and the results were shown separately. The reason was twofold: from one side, this allowed to verify the accuracy increment due to the improved capacity of the subjects to concentrate on the task; from the other side, this served to highlight the eventual modifications of the optimal reference frequencies values, both in γ and α bands, from one test to the other.

By analyzing the reported data, it can be observed that the resulting average accuracy was 88.7% for the first test and 89.9% for the second. The small accuracy increment that interested 23 out of 28 subjects from the first to the second test, though not particularly evident, was probably due to the fact that most of the subjects found easier to concentrate on the task in the second test with respect to the first, as confirmed by 26 out of 28 subjects interviewed after the second test. In fact, though they judged the task very simple from the beginning, they found a better familiarity with the second test than with the first. However, in some case the accuracy decreased from the first to the second test. The explanation of these little variations could also due to a different choice of the optimal reference frequencies in the second test with respect to the first: for some subject (for example S1.1, where accuracy increased, or S2.3, where accuracy decreased) these modifications were accompanied by a significant accuracy modification.

To exclude this possibility, we repeated the classification procedure by inverting the frequency parameters (in the first test we used the parameters previously set for the second test and vice versa) and we found that the accuracy worsen in any case (average difference: −1.6%), though the results are not shown. This confirms that: the little improvement was due to the increasing of familiarity of the subjects with the task; little modifications in frequency parameters values did not modify accuracy significantly. Moreover, though 4.5 h elapsed between the first and the second test, intra-subject changes in optimal frequency values were small.

The global average accuracy was 89.3%, the best response occurred from S2.6 (95%), the worst from S1.6 (82.8%). An important aspect is that the classification strategy used rows 4 or 7 of Table 1, giving the answer "DON'T KNOW" (indicated in Table 2 with the symbol "?") occurred very rarely (globally, 1.39% of the total trials were classified as "?"). This demonstrates that, though possible (due to the presence of experimental noise), these cases were highly improbable.

It is also important to note that the condition in Step 6 of the proposed algorithm never became false for the considered experiments. This was probably due to the fact that the experimental noise was low (electromagnetic interferences were very low, being the experiments conducted in a controlled environment, and the movements of the subjects were almost absent due to the low duration of the tests).

The obtained experimental results also demonstrated that the proposed approach and the classification method were independent of the fact that the analyzed subjects were right-handed (specific average accuracy of 89.6%) or left-handed (specific average accuracy of 88.5%). In fact, to underline this aspect and to show that the produced activation was always located on the right hemisphere of the brain, the r^2 maps of two subjects, one

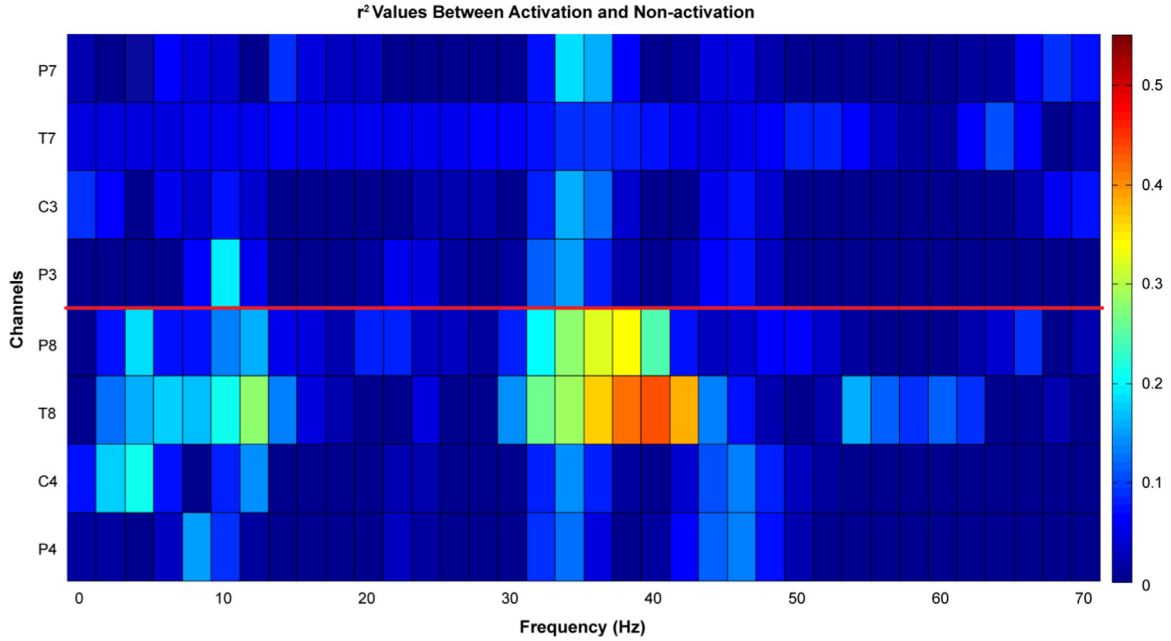

Fig. 5. Function r^2 calculated between Activation and Non-Activation on a 10-trials sequence for the subject S4.2.

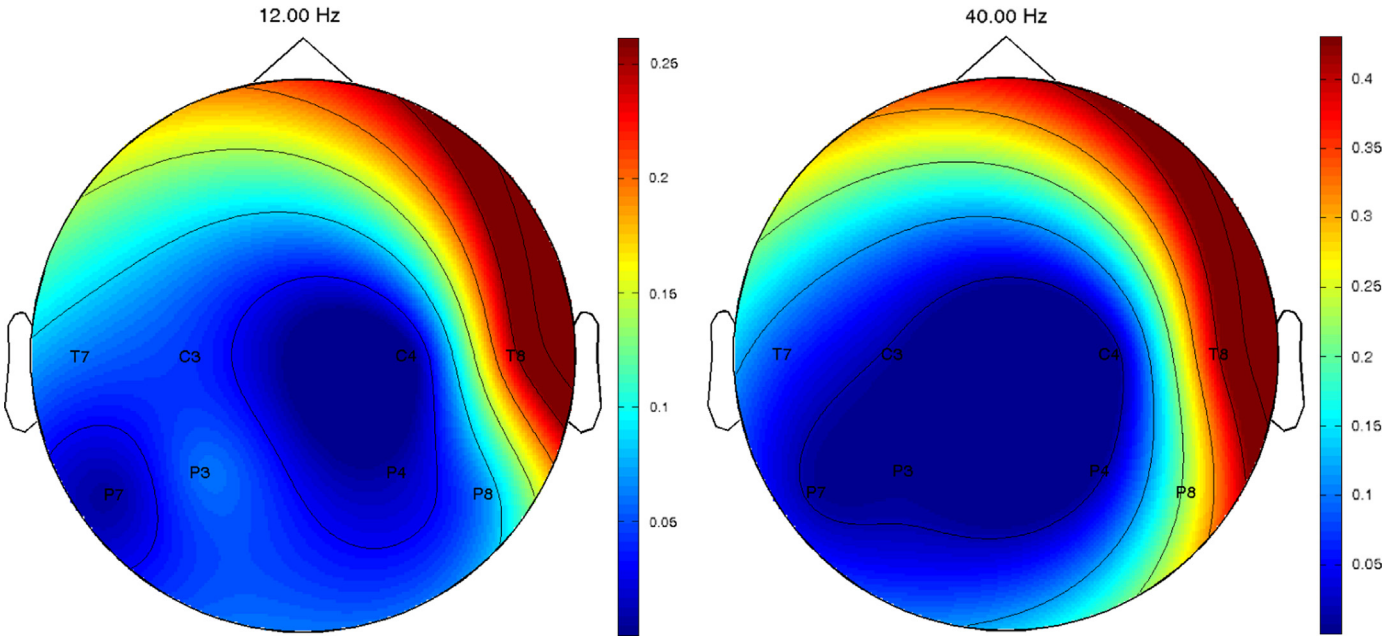

Fig. 6. Function r^2 calculated between Activation and Non-Activation on a 10-trials sequence calculated on 12 Hz (left panel) and 40 Hz (right panel) for the subject S4.2.

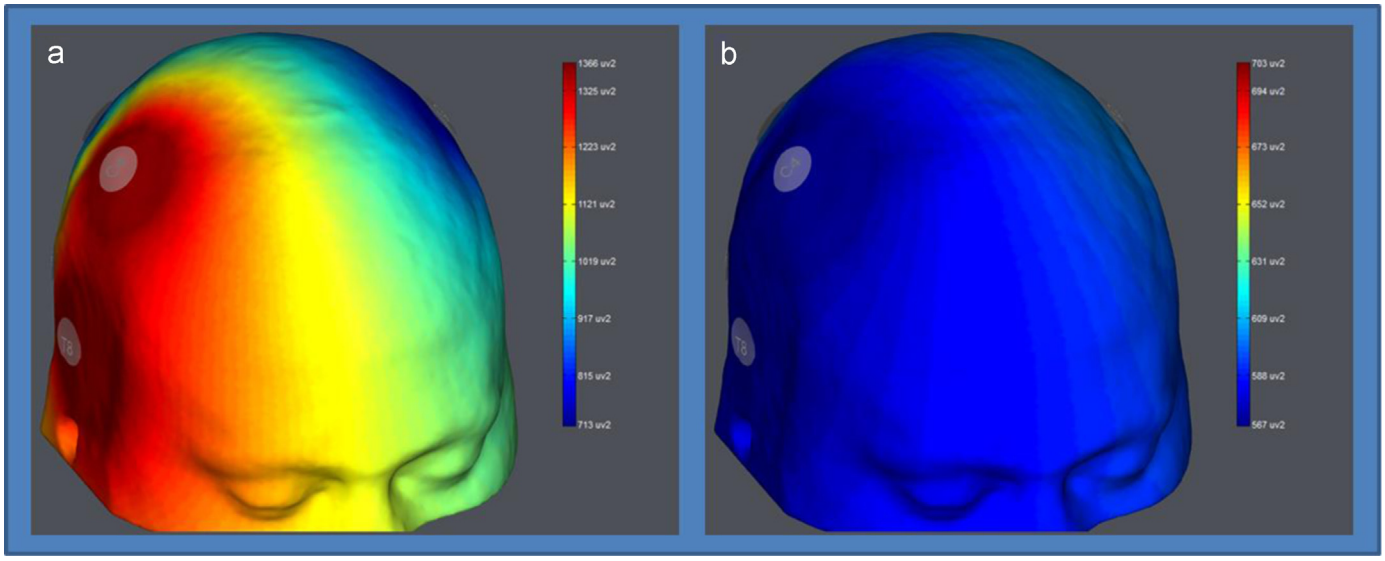

Fig. 7. Scalp maps representing the power spectrum of the signals during an Activation (a) and a Non-Activation (b) measured in the gamma band for the subject S4.2.

right-handed (S4.2) and the other left-handed (S2.5), are explicitly reported. Regarding the subject S4.2, the function r^2, calculated on a 10-trial sequence (5 arrows and 5 crosses), is shown in Fig. 5, for all channels and frequencies, and in Fig. 6, for 12 Hz and 40 Hz, respectively. For this specific subject, activations were so strong in the γ band to be directly recognizable in the signal power spectrum (r^2 would not have been necessary), as shown in Fig. 7. However, despite well distinguishable activations, the obtained accuracy was 94.4%, that is lower than 100%.

This could be due to concomitant factors: limitations of the classification strategy; changes in the optimal frequency values during the test that induced mistakes in classification; the subject did not follow the instructions of the task for the whole duration of the test. Though the first two factors are directly attributable to the classification strategy, the last was due to the subject. However, we had no way to separate the causes of the anomalous classification results. For this reason, being the accuracy calculated including all the wrongly classified datasets, it represented an underestimate of the true accuracy level. In a real implementation of a BCI that can be autonomously driven by the user, the effect of this term should be greatly reduced because the motivational boost of the subject should increase.

Regarding the subject S2.5, the corresponding results are reported in Figs. 8 and 9 (for this subject the power spectrum was not discriminant and is not shown). In both case, as for the whole set of the analyzed subjects, the activity was mainly concentrated in the γ band and in the α band of the right hemisphere of the brain.

5. Conclusions and future developments

An innovative paradigm to generate self-induced EEG signal and a binary, threshold-based, classification algorithm have been presented and used to classify disgust produced by remembering an unpleasant odor. Both the particular activation task and the proposed classification strategy are novel.

The proposed paradigm has been tested on 28 healthy subjects that found the task very simple and natural. Moreover, they learned the protocol very fast and considered it not tiring, though 55% of them

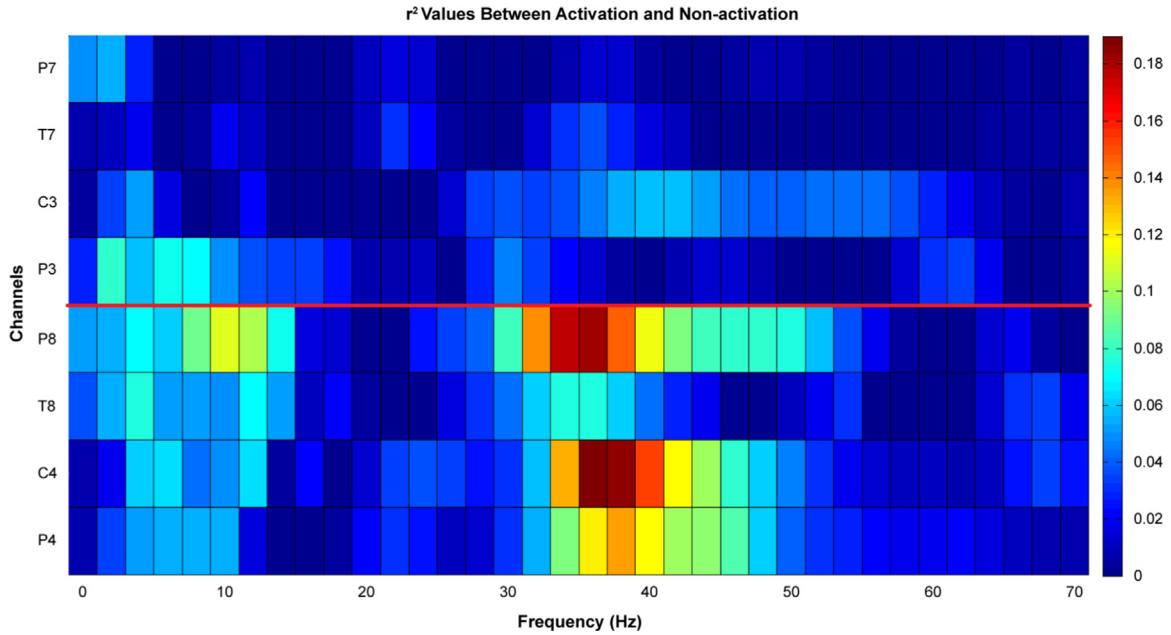

Fig. 8. Function r^2 calculated between Activation and Non-Activation on a 10-trials sequence for the subject S2.5.

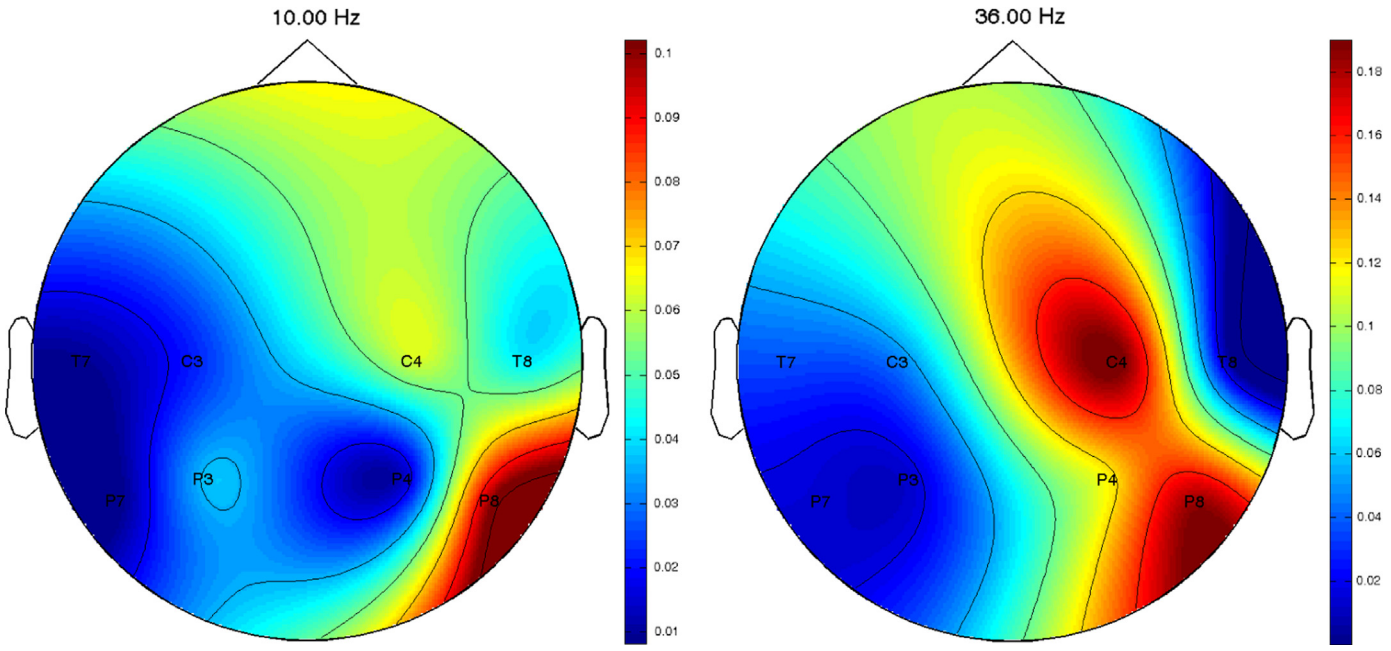

Fig. 9. Function r^2 calculated between Activation and Non-Activation on a 10-trials sequence calculated on 10 Hz (left panel) and 36 Hz (right panel) for the subject S2.5.

at the end of the tests affirmed that they were unable to maintain a high concentration level for the whole duration of the tests.

Regarding the classification strategy, it resulted effective and accurate (about 90% in the average), though the obtained value was an underestimate of the effective value. In fact, the accuracy evaluation also counted the mistakes done by the classification algorithm when examining signals with very low useful information due to the loss of concentration of the examined subjects. Though we could not quantify the contribution of this effect, we can affirm that the effective accuracy was above 90%. These good performances were mainly due to the use of the γ band, which is unusual for the great part of the commonly brain activities.

The results were independent both of the fact that the analyzed subjects were right-handed or left-handed and also that the subjects used their eyes to be synchronized with the proposed cues because we did not use the occipital channels for classification. Moreover, the symbols used were anonymous and had no affinity with the task: their presentation served just to synchronize the subjects and not for eliciting disgust or relaxation. However, due to the fact that the proposed task, besides emotive, was also both a visual stimulation and an imagination task (the subject had to observe a symbol on a computer screen and to associate it to a negative olfactory situation by remembering a really lived experience), both occipital and frontal channels were excluded from the measurements to avoid the influence of the visual and imagination components.

Future work will first be devoted in the implementation of a single trial binary BCI based on the proposed paradigm and classification algorithm. Moreover, efforts will be dedicated to use optimization algorithms, such as the common spatial pattern and its variants [39,40], as classification strategies (on the same data),

and to compare them with the proposed method both in accuracy and in efficiency. Time will be dedicated to study other well-distinguishable emotional states to work alongside the disgust to increase the number of choices. Moreover, the proposed paradigm will be tested with trials of shorter duration (here we used 3.6 s: we aim at reducing this interval to 2 s) and the system will be evaluated by using a standardized evaluation framework [41].

The obtained results are very encouraging and allow us to believe that the proposed system can became a useful, though simple, communication tool for disabled people for which other BCI paradigms are useless.

Acknowledgements

We are very grateful to the “Fondazione Fabio Sciacca Onlus” for having supported this research project.

References

[1] J.R. Wolpaw, N. Birbaumer, W.J. Heetderks, D.J. McFarland, P.H. Peckham, G. Schalk, E. Donchin, L.A. Quatrano, C.J. Robinson, T.M. Vaughan, Brain–computer interface technology: a review of the first international meeting, IEEE Trans. Rehabil. Eng. 8 (2) (2000) 164–173.
[2] J.J. Shih, D.J. Krusienski, J.R. Wolpaw, Brain–computer interfaces in medicine, Mayo Clin. Proc. 87 (3) (2012) 268–279.
[3] A. Vallabhaneni, T. Wang, B. He, Brain–computer interface, Neural Eng. (2005) 85–121.
[4] J.A. Coan, J.J.B. Allen, Frontal EEG asymmetry as a moderator and mediator of emotion, Biol. Psychol. 67 (2004) 7–49.
[5] C.S. Herrmann, M.H.J. Munk, A.K. Engel, Cognitive functions of gamma-band activity: memory match and utilization, Trends Cogn. Sci. 8 (8) (2004) 347–355.
[6] M. Li, B.L. Lu, Emotion classification based on gamma-band EEG, Proc. Ann Int. Conf. IEEE EMBS 2009 (2009) 1223–1226.
[7] I. Wickelgren, Neuroscience: tapping the mind, Science 299 (5606) (2003) 496–499.
[8] L.A. Farwell, E. Donchin, Talking off the top of your head: toward a mental prosthesis utilizing event-related brain potentials. Electroencefalogr, Clin. Neurophysiol. 70 (6) (1988) 510–523.
[9] J.R. Wolpaw, D.J. McFarland, Control of a two-dimensional movement signal by a non invasive brain–computer interface in humans, Proc. Natl. Acad. Sci. U.S. A. 101 (51) (2004) 17849–17854.
[10] C. Neuper, G.R. Muller-Putz, R. Scherer, G. Pfurtscheller, Motor imagery and EEG-based control of spelling devices and neuroprostheses, Prog. Brain Res. 159 (2006) 393–409.
[11] Y. Han, H. Bin, Brain–computer interfaces using sensorimotor rhythms: current state and future perspectives, IEEE Trans. Biomed. Eng. 61 (5) (2014) 1425–1435.
[12] A. Furdea, S. Halder, D.J. Krusienski, D. Bross, F. Nijboer, N. Birbaumer, A Kübler, An auditory oddball (P300) spelling system for brain–computer interfaces, Psychophysiology 46 (3) (2009) 617–625.
[13] A. Kübler, A. Furdea, S. Halder, E.M. Hammer, F. Nijboer, B. Kotchoubey, A brain–computer interface controlled auditory event-related potential (p300) spelling system for locked-in patients, Ann. N.Y. Acad. Sci. 1157 (2009) 90–100.
[14] G. Shangkai, W. Yijun, G. Xiaorong, H. Bo, Visual and auditory brain–computer interfaces, IEEE Trans. Biomed. Eng. 61 (5) (2014) 1436–1447.
[15] A.M. Brouwer, J.B.F. van Erp, A tactile P300 brain–computer interface, Front. Neurosci. 4 (2010) 19.
[16] G.R. Muller-Putz, R. Scherer, C. Neuper, G. Pfurtscheller, Steady-state somatosensory evoked potentials: suitable brain signals for brain–computer interfaces? IEEE Trans. Neural Syst. Rehabil. Eng. 14 (1) (2006) 30–37.
[17] G.G. Molina, T. Tsoneva, A. Nijholt, Emotional brain–computer interfaces, in: Proceedings of the 3rd International Conferrence on Affective Computing and Intelligent Interaction and Workshops, ACII, 2009, pp. 1–9.
[18] D. Nie, X.W. Wang, L.C. Shi, B.L. Lu, EEG-based emotion recognition during watching movies, in: Proceedings of the 5th International IEEE EMBS Conference On Neural Engineering, 2011, pp. 667–670.
[19] R.W. Picard, J. Klein, Towards computers that recognize and respond to user emotion: theoretical and practical implications, Interact. Comput. 14 (2) (2002) 141–169.
[20] H. Kober, L.F. Barrett, J. Joseph, E. Bliss-Moreau, K. Linquist, T.D. Wager, Functional grouping and cortical-subcortical interactions in emotion: a meta-analysis of neuroimaging studies, Neuroimage 42 (2008) 998–1031.
[21] K. Lindquist, T.D. Wagner, H. Kober, E. Bliss-Moreau, L.F. Barrett, The brain basis of emotion: a meta-analysis review, Behav. Brain Sci. 35 (2012) 121–143.
[22] A. Deak, Brain and emotion: cognitive neuroscience of emotions, Rev. Psychol. 18 (2) (2011) 71–80.
[23] K.S. Kassam, A.R. Markey, V.L. Cherkassky, G. Loewenstein, M.A. Just, Identifying emotions on the basis of neural activation, Plos One 8 (6) (2013) 1–11.
[24] T.M. Mitchell, R. Hutchinson, R.S. Niculescu, F. Pereira, X. Wang, M. Just, S. Newman, Learning to decode cognitive states from brain images, Mach. Learn. 57 (2004) 145–175.
[25] A. Choppin, EEG-based human interface for disabled individuals: emotion expression with neural networks Ph.D. dissertation, Tokyo Institute of Technology, 2000.
[26] G. Chanel, J. Kronegg, D. Grandjean, T. Pun, Emotion assessment: arousal evaluation using EEG's and peripheral physiological signals, Lect. Notes Comput. Sci. 4105 (2006) 530–537.
[27] D. Bos, EEG-based emotion recognition, 2006 [On-line]. Available: ⟨http://hmi.ewi.utwente.nl/verslagen/capita-selecta/CS-Oude_Bos-Danny.pdf⟩.
[28] Q. Zhang, M. Lee, Analysis of positive and negative emotions in natural scene using brain activity and GIST, Neurocomputing 72 (2009) 1302–1306.
[29] X.W. Wang, D. Nie, B.L. Lu, Emotional state classification from EEG data using machine learning approach, Neurocomputing 129 (2014) 94–106.
[30] C.P. Niemic, Studies of emotion: a theoretical and empirical review of psychophysiological studies of emotion, J. Undergrad. Res. 1 (2002) 15–18.
[31] R.I. Henkin, L.M. Levy, Lateralization of brain activation to imagination and smell of odors using functional magnetic resonance imaging (fMRI): left hemispheric localization of pleasant and right hemispheric localization of unpleasant odors, J. Comput. Assist. Tomogr. 25 (4) (2001) 493–514.
[32] L.M. Levy, R.I. Henkin, C.S. Lin, A. Hutter, D. Schellinger, Odor memory induces brain activation as measured by functional MRI, J. Comput. Assist. Tomogr. 23 (1999) 487–498.
[33] J. Decety, J. Grezes, The power of simulation: imagining one's own and other's behavior, Brain Res. 1079 (2006) 4–14.
[34] M. Bensafi, C. Rouby, V. Farget, M. Vigouroux, A. Holley, Asymmetry of pleasant vs. unpleasant odor processing during affective judgment in humans, Neurosci. Lett. 328 (2002) 309–313.
[35] ⟨http://www.neuroelectrics.com/enobio⟩.
[36] V. Jurcak, D. Tsuzuki, I. Dan, 10/20, 10/10, and 10/5 systems revisited: Their validity as relative head-surface-based positioning systems, Neuroimage 34 (2007) 1600–1611.
[37] ⟨http://www.mathworks.com⟩.
[38] ⟨http://www.schalklab.org/research/bci2000⟩.
[39] B. Blankertz, R. Tomioka, S. Lemm, M. Kawanabe, K.R. Muller, Optimizing spatial filters for robust EEG single-trial analysis, IEEE Signal Process. Mag. 25 (1) (2008) 41–56.
[40] P. Xu, T. Liu, R. Zhang, Y. Zhang, D. Yao, Using particle swarm to select frequency band and time interval for feature extraction of EEG based BCI, Biomed. Signal Process. Control 10 (2014) 289–295.
[41] M. Billinger, C. Brunner, R. Scherer, A. Holzinger, G.R. Muller-Putz, Towards a framework based on single trial connectivity for enhancing knowledge discovery in BCI, Lect. Notes Comput. Sci. 7669 (2012) 658–667.

Giuseppe Placidi received the Master of Science in Computer Science in 1991 and the Ph.D. degree in Medical Imaging both at the University of L'Aquila. Since 2005 he has been an assistant professor in Computer Science in the Department of Life, Health & Environmental Sciences. His research interests include medical imaging, signal and image analysis, computer vision, artificial intelligence in medicine, pattern recognition. He is an Editorial Board member of international journals and is author of more than 100 publications, 8 patents, and 1 book.

Danilo Avola is research engineer of computer science at the University of L'Aquila since 2011. Prior to that, he was on the Sapienza University and National Research Council. He received his degree in Computer Science from the Sapienza University and the Ph.D. in Molecular and Ultrastructural Imaging from University of L'Aquila. His research interests include Human Computer Interaction, Computer Vision, Signal Processing, Machine Learning, Image and Video Processing, and Pattern Recognition. He serves on the Steering Committee of selected International Conferences and is an Editorial Board member of different International Journals. His publications have appeared in Elsevier, ACM, IEEE, and Springer.

Andrea Petracca received the Master Degree in Computer Science from University of L'Aquila in October 2013. He is is currently a Ph.D. student of the Department of Life, Health and Environmental Sciences at University of L'Aquila. His research interests include medical imaging, signal and image processing, software engineering, and machine learning.

Fiorella Sgallari is currently professor of Numerical Analysis at the University of Bologna. She is author of more than 120 publications. Her research concerns PDE models and numerical methods for image processing and solution of very large linear systems arising from discrete ill posed problems. She was scientific coordinator of national, international and industrial projects. She organized workshops and international conferences. She is Associate Editor of international journals. From 2003 she joined the Ph.D. Committee in Mathematics, University of Bologna. From 2006 to 2013 she was Chair of C.I.R.A.M. – Research Centre of Applied Mathematics, University of Bologna.

Matteo Spezialetti received the Master Degree in Computer Science from the University of L'Aquila in 2014. His actual position is of research contractor of the Department of Life, Health and Environmental Sciences at University of L'Aquila. His research interests include image processing, signal analysis, pattern recognition, and machine learning.